Biophysical Chemistry 165–166 (2012) 30–38

Contents lists available at SciVerse ScienceDirect

Biophysical Chemistry

journal homepage: http://www.elsevier.com/locate/biophyschem

Mechanism of inactivation of ocriplasmin in porcine vitreous

Frans Aerts [a,1], Bernard Noppen [a,1], Laetitia Fonteyn [a], Rita Derua [b], Etienne Waelkens [b], Marc D. de Smet [c], Marc Vanhove [a,*]

[a] Thrombogenics N.V., Gaston Geenslaan 1, 3001 Leuven, Belgium
[b] Laboratory of Phosphoproteomics, Department of Molecular Cell Biology, Campus Gasthuisberg O&N1, K.U. Leuven, Herestraat 49, bus 901, B-3000 Leuven, Belgium
[c] MIOS sa, Retina and Inflammation Service, Lausanne, Switzerland

HIGHLIGHTS

- Microplasmin is being developed for the treatment of symptomatic vitreomacular adhesion.
- Microplasmin rapidly inactivates in porcine vitreous.
- Inactivation results from autolysis and is concentration-dependent.
- Autolytic cleavage occurs at a limited number of sites.
- Autolysis requires at least partial or local unfolding.

GRAPHICAL ABSTRACT

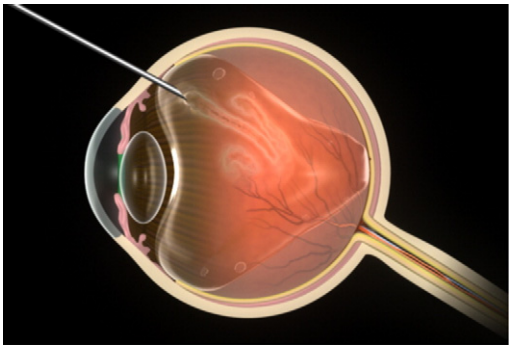

ARTICLE INFO

Article history:
Received 9 February 2012
Accepted 1 March 2012
Available online 8 March 2012

Keywords:
Ocriplasmin
Symptomatic vitreomacular adhesion
Posterior vitreous detachment
Autolysis
Local or partial unfolding

ABSTRACT

Ocriplasmin, a 249-amino acid recombinant C-terminal fragment of human plasmin, has the potential to degrade, within the eye, the protein scaffold that links the vitreous to the retina. This may be beneficial to the treatment of a number of important ophthalmic indications, such as symptomatic vitreomacular adhesion. We demonstrate here that ocriplasmin used at therapeutically-relevant concentrations is inactivated in porcine vitreous through autolytic degradation. Autolytic cleavage occurs at a limited number of sites, primarily K156–E157, K166–V167 and R177–V178, which, as predicted, contain a positively-charged arginine or lysine residue at the P1 position. Our data also suggest that autolytic degradation requires at least local or partial unfolding of the protein.

1. Introduction

The use of plasmin, the enzyme that degrades fibrin polymers, has been envisioned for human therapy since the 1950s [6]. However, production of recombinant plasminogen (the precursor of plasmin) in eukaryotic systems proved difficult, in part due to the presence of intracellular plasminogen activators [31]. Researchers therefore focused on the production of shorter derivatives of plasmin which retain fibrinolytic activity.

Ocriplasmin (des-kringle 1–5 plasmin), also known as microplasmin, is a truncated form of plasmin. Originally shown to form upon autolytic degradation of plasmin at high pH, ocriplasmin exhibits intact catalytic activity while lacking all 5 kringle domains [32]. It is however only in the early 2000s that expression of recombinant microplasminogen (the inactive zymogen of ocriplasmin) with high yield in the methylotrophic yeast *Pichia pastoris*, followed by purification, activation with recombinant staphylokinase and formulation as a stable product [18] allowed the exploration of its therapeutic use.

* Corresponding author. Tel.: +32 16 751 322; fax: +32 16 751 311.
E-mail address: marc.vanhove@thrombogenics.com (M. Vanhove).
[1] These authors contributed equally to this work.

0301-4622/$ – see front matter © 2012 Elsevier B.V. All rights reserved.
doi:10.1016/j.bpc.2012.03.002

Symptomatic vitreomacular adhesion (VMA) is a condition where age-related posterior vitreous detachment (PVD), i.e. separation of the posterior hyaloid from the inner limiting membrane, is incomplete. When this occurs, vitreous traction induces visual distortions (i.e. metamorphopsia). VMA can also induce a localized retinal tear or hole (macular hole) and permanent loss of vision. Vitreous traction can be relieved through a surgical procedure known as vitrectomy. However, this procedure carries the risk of damage to the retinal surface or the optic nerve head [12,29]. Hence, a number of enzymes have been tested for induction of enzymatic rather that surgical PVD [4,23,27,28]. Among these, plasmin has been shown to induce PVD in both animal models [9,14,30] and post-mortem human eyes [10,16], and a similar activity was demonstrated for ocriplasmin shortly after it became available [11]. Ocriplasmin is currently under investigation for the intra-ocular treatment of VMA, and clinical trial data indicate that ocriplasmin is able to induce posterior vitreous detachment in VMA patients.

In its active form, ocriplasmin (M.W. 27,237 Da) consists of two polypeptide chains of 19 and 230 residues linked by two disulfide bonds joining residues 6 and 124, and 16 and 24. The 230-residue polypeptide is further stabilized by 4 intra-chain disulfide bonds (Fig. 1). Although stable in its formulation buffer, it was recognized early that ocriplasmin has limited stability once injected in the vitreous cavity. In this paper, inactivation of ocriplasmin in porcine vitreous was characterized from a kinetic and mechanistic standpoint. We demonstrate here that inactivation of ocriplasmin results from autolytic degradation.

2. Materials and methods

2.1. Materials

Porcine eyes were collected at the Rima n.v. slaughterhouse (Mechelen, Belgium), and transported on ice to the site of experimentation. The vitreous from individual eyes was collected and homogenized by flushing it twice through a 5 ml syringe and then three to five times through a 5 ml syringe capped with a 18 G × 1 ½″ needle. The homogenized vitreous was then centrifuged at 4 °C for 5 min at 12,000 *g*, the supernatant was collected and the pellet discarded. D-Val-Phe-Lys chloromethyl ketone came from Calbiochem (cat. 627624). Ocriplasmin used in this study was clinical-grade material. The recombinant protein was produced in *P. pastoris* in the form of the precursor microplasminogen. The protein was recovered from the fermentation medium and purified using classical chromatography steps using orthogonal separation modes. Microplasminogen was then activated to the active protease (ocriplasmin) using an activation resin. Following activation, process impurities were reduced by a further chromatography stage. The purified ocriplasmin was formulated in formulation buffer, filtered and stored.

2.2. Activity measurements

The hydrolytic activity of ocriplasmin was measured using the chromogenic substrate S-2403 (L-pyroglutamyl-L-phenylalanyl-L-lysine-p-nitroaniline hydrochloride, Chromogenix, Milano, Italy, cat. 822254-39) by monitoring the initial rate of p-nitroaniline release at 405 nm. Unless otherwise stated, measurements were performed at 37 °C in 50 mM Tris–HCl, 38 mM NaCl, 0.01% Tween-80, pH 7.4 with the help of a PowerWave microplate reader (Biotek, KC4 software). S-2403 was used at a concentration of 0.3 mM, and the final ocriplasmin concentration in the assay was typically in the 1–10 nM range.

Residual molar concentrations of active ocriplasmin in vitreous or neutral-pH buffer were calculated from activity measurements by comparing the measured activities with the hydrolytic activities determined for reference samples of known concentration. Inactivation of ocriplasmin in buffer or eye vitreous was measured at 37 °C.

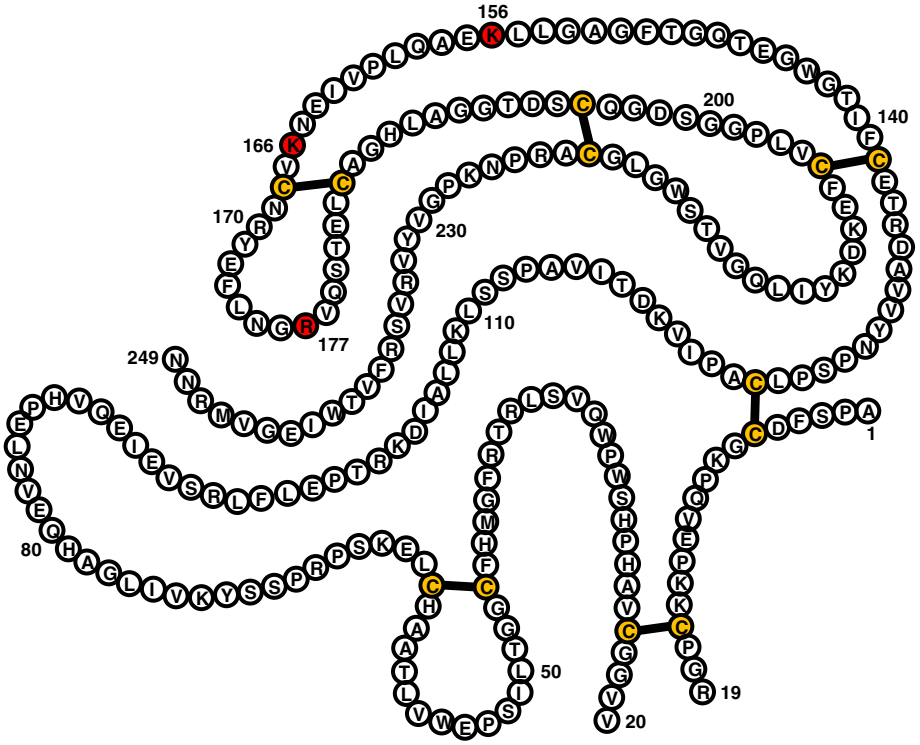

Fig. 1. Primary structure of active ocriplasmin.Active ocriplasmin consists of 2 polypeptides of 19 and 230 residues. The cysteine residues are highlighted in orange, and the positions of the six disulfide bonds are indicated. Lysine 156, lysine 166 and arginine 177 are highlighted in red.

2.3. SDS-PAGE and western-blots

SDS-PAGE was performed using NuPAGE 4–12% Bis-Tris gels (Invitrogen, cat. NP0335BOX), following the manufacturer's recommendations. The gels were stained using the Simply Blue SafeStain from Invitrogen (cat. LC6060). For western-blots, proteins were transferred to nitrocellulose membranes using the iBlot Gel Transfer device (Invitrogen, cat. IB1001EU) and iBlot Gel Transfer Stacks (Invitrogen, IB3010-02). Following blocking with the Superblock T20 Blocking Buffer (Thermo Scientific, cat. 37516), ocriplasmin was detected using 7H11A11 (1 μg/ml), a murine monoclonal antibody obtained by immunizing Balb/c mice with recombinant ocriplasmin, followed by a goat anti-mouse IgG HRP-labeled (Thermo Scientific, cat. 32430). HRP activity was revealed using the SuperSignal West Dura chemiluminescent substrate (Thermo Scientific, cat. 34076), combined with a BioSpectrum imaging system (UVP).

2.4. HPLC

HPLC analyses were performed using an Acquity UPLC instrument (Waters). The samples were diluted 5-fold in 0.1% trifluoroacetic acid (TFA), 5% acetonitrile, and 6 μl of the diluted samples were injected on a BEH300 C18 Acquity UPLC column (Waters) pre-equilibrated in 0.1% TFA, 34% acetonitrile. Elution was performed by applying a 34 to 44% acetonitrile, 1.5-ml linear gradient in 0.1% TFA, and the proteins were detected by following the absorbance at 214 nm. The flow rate was 100 μl/min, and the temperature of the column was maintained at 75 °C.

2.5. N-terminal sequencing

N-terminal sequencing of bands excised from SDS-gels was performed by Eurosequence B.V., Groningen, The Netherlands.

2.6. Mass spectrometry

Autolytic degradation of ocriplasmin (20 μM) was allowed to occur at 37 °C for 5 h in 25 mM sodium phosphate, pH 7.2, and the reaction was stopped by the addition of one volume of 0.2 M acetic acid. The sample was subsequently treated with Tris(2-carboxyethyl) phosphine hydrochloride (final concentration 50 mM) for 1 h at room temperature to enable reduction of the disulfide bridges. Prior to analysis, the sample was further diluted two times in 50% acetonitrile in HPLC grade water. Mass spectrometry analysis was performed on an ABI 4800 MALDI TOF/TOF mass spectrometer running in linear mode with positive ionization. 4-hydroxy-alpha-cyano-cinnamic acid (5 mg/ml in 50% acetonitrile/0.1% trifluoroacetic acid) was used as a matrix. Mass range was set to 5–30 kDa in order to detect both the intact protein and its autolytic fragments.

3. Results

3.1. Ocriplasmin is rapidly inactivated in homogenized porcine vitreous in a dose-dependent fashion

Different doses of ocriplasmin (ranging from 50 to 250 μg) were injected into homogenized vitreous recovered from individual porcine eyes. Under these conditions, the enzyme was rapidly inactivated (Fig. 2A). Furthermore, the rate of inactivation increased with the dose; e.g. the percentage of initial activity decreased from 43 ± 4 to 21 ± 7 after 7 h, and from 29 ± 5 to 8 ± 4 after 24 h for the 50 and 250 μg doses, respectively.

3.2. Inactivation of ocriplasmin in vitreous follows a second-order process

The observation that ocriplasmin loses its activity in a concentration-dependent manner once diluted in vitreous suggests that inactivation

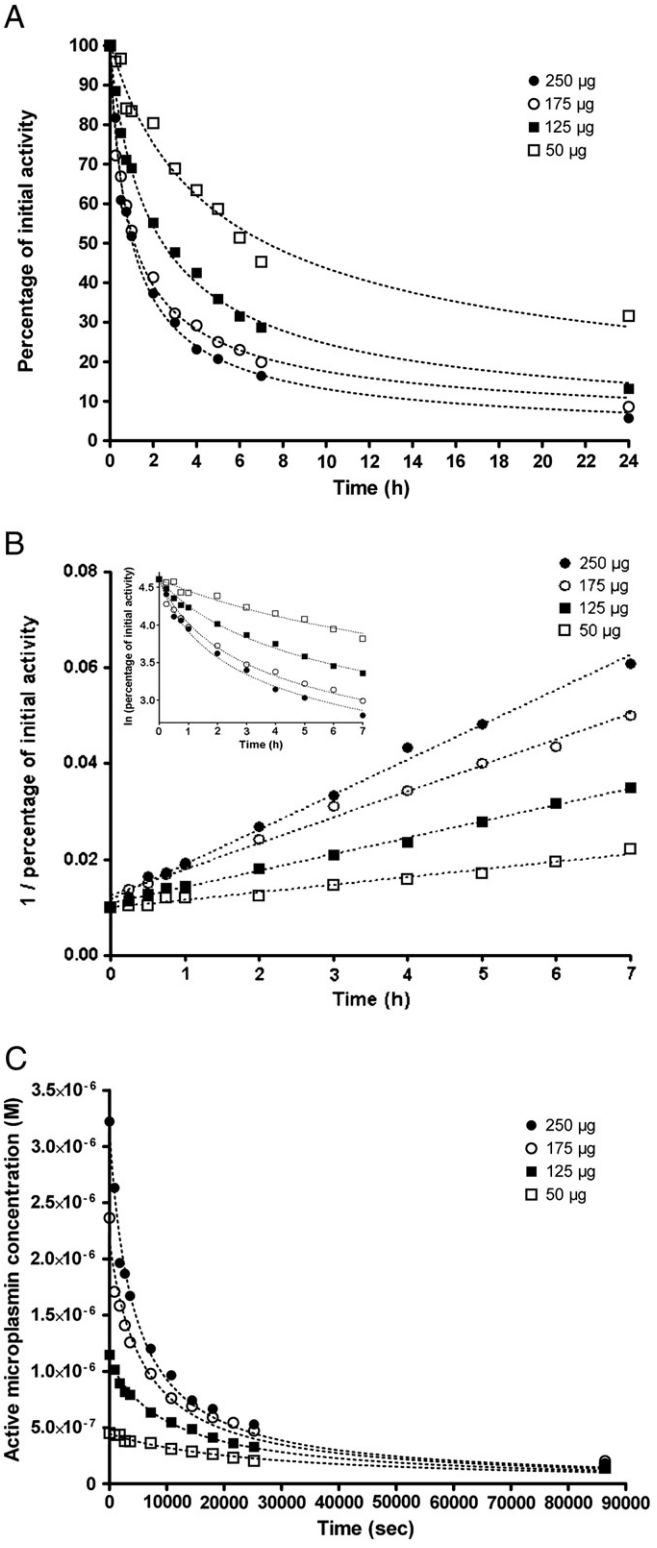

Fig. 2. Inactivation of ocriplasmin in porcine vitreous obeys second-order kinetics. (A) Representative data for the inactivation of ocriplasmin in homogenized porcine vitreous. Different doses of ocriplasmin (50, 125, 175 and 250 μg) were added to homogenized vitreous recovered from individual porcine eyes, and hydrolytic activity was measured at various time points. The volume of vitreous was 3.0, 2.5, 2.1 and 2.4 ml for the 50, 125, 175 and 250 μg doses, respectively. The dotted lines were drawn to aid visualization. (B) Data from Fig. 2A linearized assuming a second-order reaction, i.e. by plotting (1/percentage of initial activity) vs. time. The inset shows the natural logarithm of the percentage of initial activity vs. time. The dotted lines were drawn to aid visualization. (C) Molar concentrations of active ocriplasmin calculated from hydrolytic activity measured at various time points (from the data of Fig. 2A). The dotted lines represent the best fits with Eq. (1).

does not occur through a monomolecular (first-order) process. This was confirmed by the non-linearity of the natural logarithm of the activity vs. time plots. By contrast, the inactivation data could be linearized assuming a second-order process, i.e. by plotting (1/percentage of initial activity) vs. time (Fig. 2B). Therefore, the activities measured at various time points were converted into molar concentrations and the concentration vs. time curves were analyzed with Eq. (1), which represents a second-order process (Fig. 2C). Eq. (1) was obtained after rearranging $1/C = 1/C_0 + k.t$ so that concentration vs. time plots can be directly analyzed by non-linear regression. This analysis led to a second-order rate inactivation constant of $81 \pm 15\ M^{-1}\ s^{-1}$.

$$C = C_0/(1 + C_0.k.t) \quad (1)$$

In Eq. (1), C_0 and C are the molar concentrations of active ocriplasmin at time 0 and time t, respectively, t is the time (expressed in s) and k is the second-order rate constant (expressed in $M^{-1}\ s^{-1}$).

3.3. Inactivation of ocriplasmin in neutral-pH buffer and vitreous obeys similar kinetics

We found that the behavior of ocriplasmin in a neutral-pH buffer (e.g. PBS) is similar to that observed in vitreous, i.e. inactivation is fast, concentration-dependent, and obeys second-order kinetics (Fig. 3). We therefore speculated that ocriplasmin inactivates through an identical mechanism both in neutral-pH buffer and in vitreous. Inactivation, however, was found to be somewhat faster in PBS, with a second-order rate constant of $176 \pm 18\ M^{-1}\ s^{-1}$.

3.4. Inactivation of ocriplasmin in neutral-pH buffer and vitreous is caused by autolysis

Autolysis of various proteases (including plasmin) has been reported to obey second-order kinetics [15,24–26]. Stoner et al. [26] proposed a two-step model for the autolysis of proteases, where the first step consists of an equilibrium between native (N) and unfolded (U) protease, while the second involves the cleavage of an unfolded protease molecule by a native molecule.

$$N \leftrightarrow U \quad (\text{Reaction1})$$

$$U + N \rightarrow \text{Fragments} + N \quad (\text{Reaction2})$$

Stoner et al. indicate that the above model leads to either first order kinetics if the rate of unfolding in Reaction 1 (i.e. the $N \rightarrow U$ step) is limiting, or to second-order kinetics if the catalytic lysis of the peptide bonds is limiting. In the latter case, Stoner et al. demonstrate that the apparent second-order rate constant k is given by Eq. (2), where k_{cat}/K_m is the catalytic efficiency of the enzyme towards itself (assuming Michaelis–Menten kinetics) and $K_{unfolding}$ is the equilibrium constant of Reaction 1 in the above model ($K_{unfolding} = [U]/[N]$).

$$k = (k_{cat}/K_m).K_{unfolding} \quad (2)$$

We considered the possibility that ocriplasmin's loss of activity was caused by autolysis both in neutral-pH buffers and in vitreous. This hypothesis was first tested using SDS-PAGE under reducing conditions. Inactivation of ocriplasmin in PBS resulted in the accumulation of two major degradation fragments of ~17 and ~10 kDa, respectively (Fig. 4A). These two fragments were not detectable under non-reducing conditions, indicating that they were linked by one or more disulfide bond(s). Ocriplasmin degradation could also be visualized by western blot, with the monoclonal antibody 7H11A11 detecting an ~17 kDa fragment (Fig. 4B), and by HPLC with the accumulation of two major species with elution times in the 9.0–9.5 min range (Fig. 4C). It should be appreciated here that HPLC analysis was performed without reduction of the

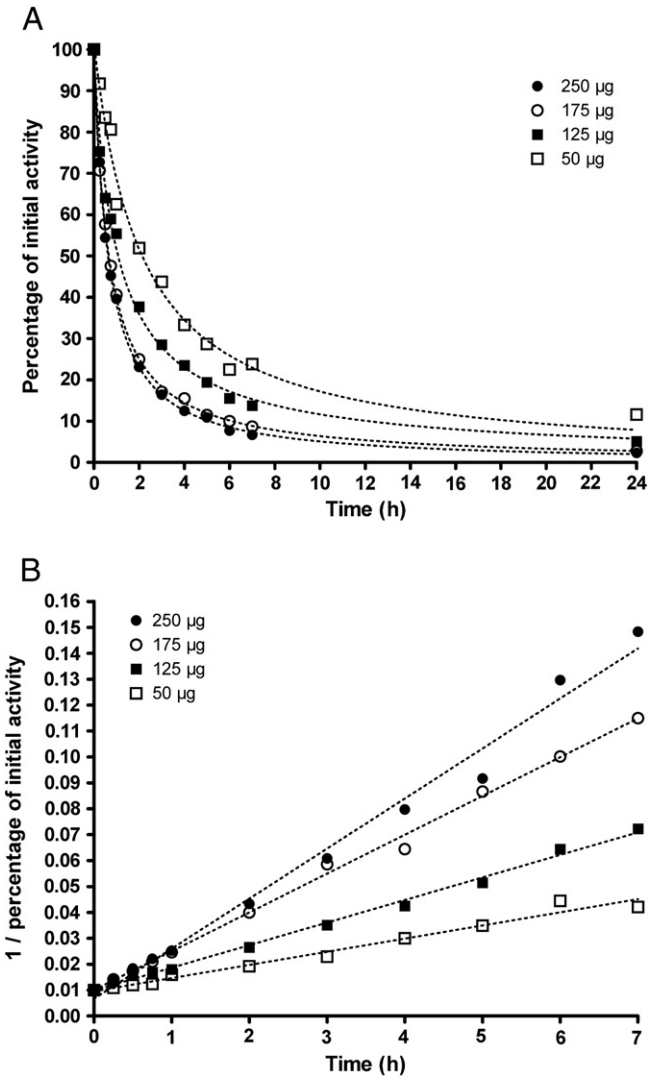

Fig. 3. Ocriplasmin inactivates in a similar manner in a neutral-pH buffer and in vitreous.(A) Inactivation of ocriplasmin in neutral-pH buffer (PBS). Different doses of ocriplasmin (50, 125, 175 and 250 µg) were diluted in PBS, and hydrolytic activity was measured at various time points. The volume of PBS was 3.0, 2.5, 2.1 and 2.4 ml for the 50, 125, 175 and 250 µg doses, respectively, in order to match the data obtained in vitreous (Fig. 2A). The dotted lines were drawn to aid visualization. (B) Data from Fig. 3A linearized assuming a second-order reaction, i.e. by plotting (1/percentage of initial activity) vs. time.

disulfide bonds, which means that the two species that accumulate over time in PBS (indicated by the arrows in Fig. 4C) are distinct from the fragments detected by reducing SDS-PAGE. Instead, they represent ~27 kDa species that differ in the position of the autolytic cleavage site(s). The shift in the ratio of the two peaks over time also indicates that one species forms first, and is then slowly converted into the other. Importantly, the kinetics of degradation as assessed by HPLC correlated well with the loss of activity (Fig. 4D), indicating that cleavage of the peptide chain results in the formation of an inactive species. Finally, degradation by autolysis was confirmed unambiguously by demonstrating that the process was prevented by the plasmin inhibitor D-Val-Phe-Lys chloromethyl ketone (Fig. 5). The inhibited enzyme exhibited a slightly modified elution time (Fig. 5C), but no autolytic fragments could be detected in this sample.

Importantly, we demonstrated, as suggested by the kinetic analysis, that inactivation of ocriplasmin in porcine vitreous also results from an autolytic process. Western blot analysis showed the appearance of a

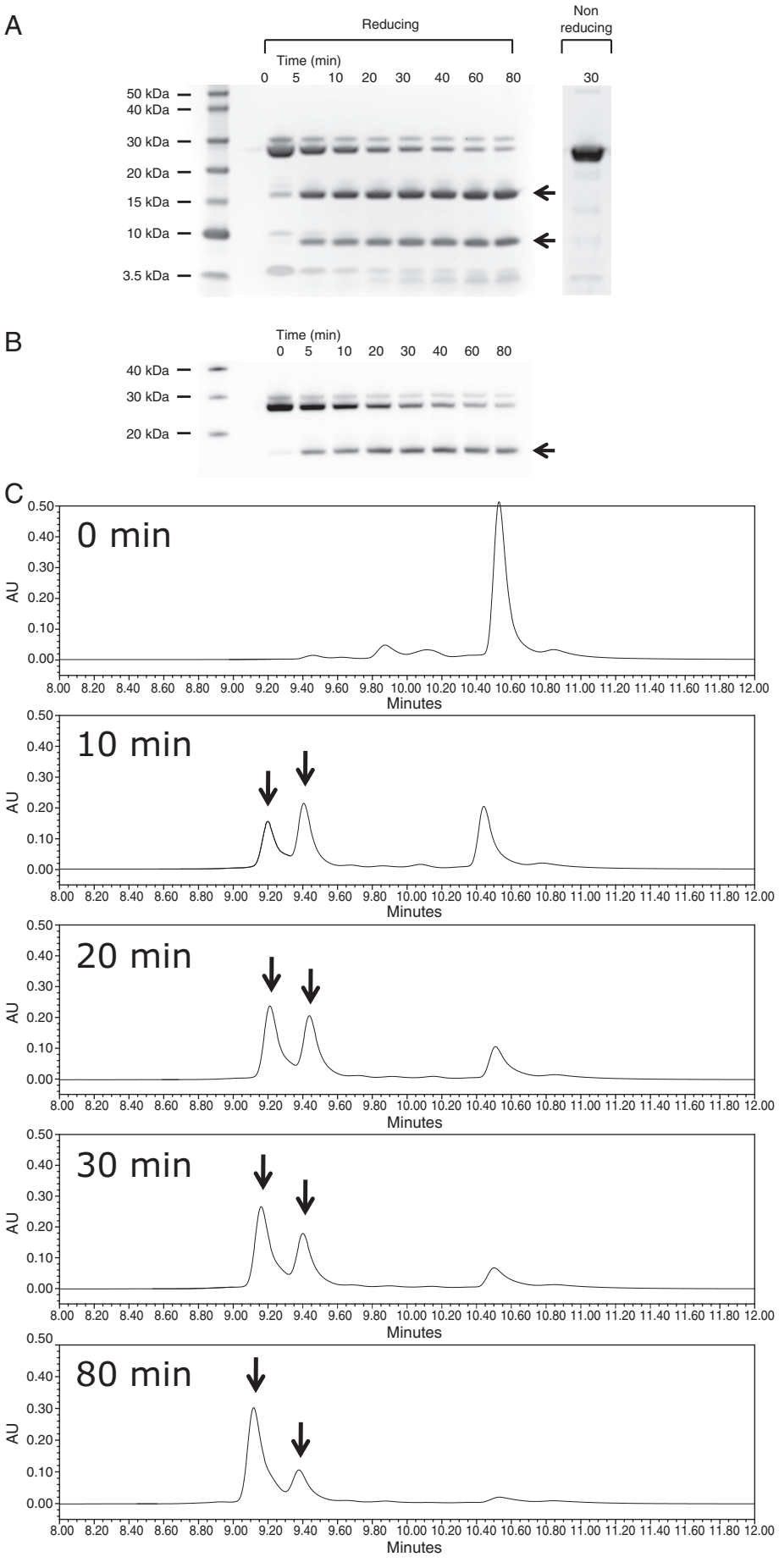
A
Reducing
Non reducing
Time (min)
0 5 10 20 30 40 60 80
30
50 kDa
40 kDa
30 kDa
20 kDa
15 kDa
10 kDa
3.5 kDa
B
Time (min)
0 5 10 20 30 40 60 80
40 kDa
30 kDa
20 kDa
C
0 min
10 min
20 min
30 min
80 min
AU
Minutes
0.00 0.10 0.20 0.30 0.40 0.50
8.00 8.20 8.40 8.60 8.80 9.00 9.20 9.40 9.60 9.80 10.00 10.20 10.40 10.60 10.80 11.00 11.20 11.40 11.60 11.80 12.00

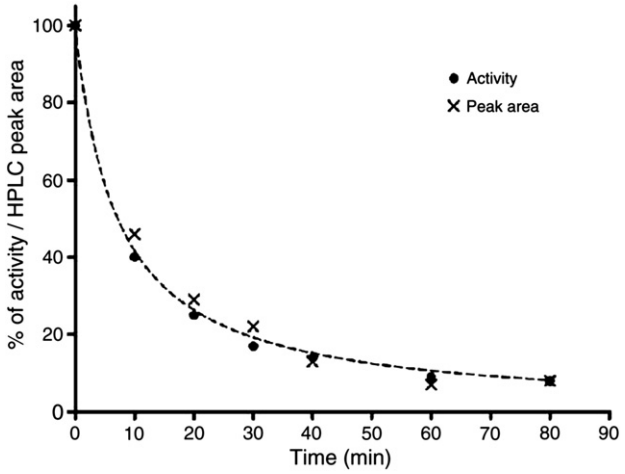

Fig. 4 (*continued*).

degradation fragment which was undistinguishable from the species generated in PBS, and no degradation was detected in the presence of D-Val-Phe-Lys chloromethyl ketone (Fig. 6).

3.5. Effect of sucrose on the rate of microplasmin autolysis

If autolysis involves partial unfolding of the protease as suggested by the model of Stoner et al., then solutes that increase the thermodynamic stability of proteins, such as sugars, should lead to a decrease in the equilibrium concentration of unfolded protease, which in turn should translate into a decreased rate of autolysis.

We tested this hypothesis using sucrose as a stabilizing agent, as it has no detectable effect on the intrinsic activity of ocriplasmin in the concentration range used here (Fig. 7A). As expected, the rate of ocriplasmin autolysis decreased significantly in the presence of increasing concentrations of sucrose (Fig. 7A), inactivation being ~12 times slower in the presence of 1 M sucrose. Since $K_{unfolding}$ in Eq. (2) is related to $\Delta G^0_{unfolding}$, the Gibbs free energy of unfolding [$\Delta G^0_{unfolding} = -RT \ln(K_{unfolding})$], it is possible to derive Eq. (3), which allows the calculation of the $\Delta\Delta G_{unfolding}$, i.e. the increase in ocriplasmin's thermodynamic stability for a given sucrose concentration. In Eq. (3), k_S and k_0 are the rates of autolysis measured in the presence and absence of sugar, respectively, R is the gas constant and T the temperature. Fig. 7B shows that $\Delta\Delta G_{unfolding}$ increased linearly with the sucrose concentration, to reach a value of 1.5 kcal/mol (6.3 kJ/mol) at 1 M sucrose. Similar findings were made using mannitol as a stabilizing agent, leading to a $\Delta\Delta G_{unfolding}$ value of ~1.3 kcal/mol (5.4 kJ/mol) at a sugar concentration of 1 M.

$$\Delta\Delta G_{unfolding} = -RT \ln(k_s/k_0) \quad (3)$$

In order to fully validate the reasoning described above, we also decided to verify that the effect of sucrose and mannitol was not due to an increase in the viscosity of the solution, although this seemed unlikely since this would indicate that the autolytic process is controlled by diffusion, and the rate of diffusion-controlled reactions, even for macromolecules, is orders of magnitude higher than the rate of ocriplasmin autolysis (10^9–10^{10} $M^{-1}\,s^{-1}$ vs. ~200 $M^{-1}\,s^{-1}$, see e.g. [3]). Instead, as proposed by Stoner and co-workers (see above), it is more likely that autolysis is limited by the cleavage of the peptide bonds. In order to demonstrate this experimentally, we followed the autolysis of ocriplasmin in the presence of benzamidine, a molecule that behaves as a competitive inhibitor of plasmin, with a reported Ki value of 0.35 mM for plasmin [17] and 0.3 mM for ocriplasmin (our own data). In essence, the use of benzamidine allowed us to tune the hydrolytic activity of ocriplasmin while maintaining all other parameters, including viscosity, unchanged. Not surprisingly, we observed that autolysis of ocriplasmin was slowed down in the presence of concentrations of benzamidine (0.3–0.9 mM, i.e. 1–3×Ki) which only partially inhibit ocriplasmin. This finding demonstrates unambiguously that autolytic degradation is limited by the rate of peptide bond cleavage.

3.6. Autolytic cleavage occurs between residues K156–E157, K166–V167 and R177–V178

Autolysis of ocriplasmin leads to the formation of two major degradation fragments as assessed by SDS-PAGE, although micro-heterogeneity detected by HPLC indicates the existence of more than one autolytic cleavage site. In order to identify the sites of cleavage, the ~17 kDa and ~10 kDa bands resolved on SDS-gel were collected and submitted to N-terminal sequencing. The ~17 kDa fragment contained the sequence Val-Val-Gly-Gly-Xaa-Val (with Xaa unidentified amino acid), which corresponds to the N-terminus of the intact 230-residue polypeptide. Sequencing of the ~10 kDa fragment yielded Val-Gln-Ser-Thr-Glu-Leu, with Xaa-Xaa-Asn-Arg-Tyr-Xaa as a minor sequence. The former sequence starts at Val178 and the latter at Val167, which indicates a cleavage between Lys166 and Val167, and between Arg177 and Val178. Cleavage at these two positions was confirmed by mass spectrometry, with the detection of two species of 7720 and 9073 Da, corresponding to a Val178→C-terminus fragment (expected mass: 7718 Da) and a Val167→C-terminus fragment (expected mass: 9070 Da), respectively. Mass spectrometry revealed the presence of a third species of 15,035 Da which can be identified as a N-terminus of the 230-residue polypeptide→Lys156 fragment (expected mass: 15,030 Da), which suggests that autolytic cleavage also occurs between Lys156 and Glu157.

4. Discussion

Ocriplasmin is capable of degrading a variety of structural proteins, such as fibrin clots [8], laminin and fibronectin, with the latter two proteins localized at the vitreoretinal interface where they are believed to play a major role in vitreoretinal attachment [5,13]. Ocriplasmin was shown in several clinical studies to induce posterior vitreous detachment [2,7]. In two recent multicenter, randomized, placebo-controlled Phase III studies referred to as TG-MV-006 and TG-MV-007 and designed to evaluate ocriplasmin for the treatment of symptomatic vitreomacular adhesion, the primary endpoint (non-surgical resolution of vitreomacular adhesion) was met for 26.5% of the patients vs. 10.1% for the patients who received a placebo injection ($p<0.001$, pooled results of the TG-MV-006 and TG-MV-007 trials).

Ocriplasmin is only moderately stable when injected in vitreous. We demonstrate here that inactivation of ocriplasmin in both neutral-pH buffer and porcine vitreous is exclusively due to autolytic degradation. The slower inactivation observed in vitreous ($k = 81\ M^{-1}\,s^{-1}$ vs. $176\ M^{-1}\,s^{-1}$ in PBS) might be attributed to the presence of species which interact with ocriplasmin, which would translate into a higher K_m and a corresponding decrease in the rate of autolysis (Eq. (2)). Alternatively, the vitreous may contain solutes that increase ocriplasmin's

Fig. 4. Inactivation of ocriplasmin in PBS is due to autolysis.Ocriplasmin was diluted in PBS to a final concentration of 18.4 μM, and autolysis was followed by SDS-PAGE, western blot and HPLC. (A) Reducing SDS-PAGE (5 μg loaded). Proteins were visualized by Coomassie staining. The arrows indicate the position of the ~17 and ~10 kDa autolytic fragments. The last lane shows analysis under non-reducing conditions of material obtained after a 30-min incubation. (B) Western blot (1 μg loaded). Ocriplasmin was detected using the 7H11A11 monoclonal antibody. The arrow indicates the ~17 kDa autolytic fragment. (C) HPLC (0.6 μg injected). Peaks corresponding to species formed upon autolytic degradation are indicated by an arrow. (D) Disappearance of the intact ocriplasmin species in HPLC is concomitant with the loss of activity.

thermodynamic stability, thereby leading to the presence of a lower concentration of the unfolded, autolysis-sensitive species at equilibrium.

As predicted for an autolytic process, inactivation of ocriplasmin follows second-order kinetics. Inactivation is therefore concentration-dependent, with faster inactivation observed at higher doses. Considering an average volume of vitreous of 4.5 ml for a human eye, a dose of 125 μg per eye as used in the TG-MV-006 and TG-MV-007 trials, and an autolytic rate constant of 81 M^{-1} s^{-1}, it is anticipated that the residual concentration of ocriplasmin will have been reduced to 50% after ~3.5 h and to 10% after ~30 h.

Detectable autolytic cleavage is restricted to only three positions (K156–E157, K166–V167 and R177–V178). All three cleavage sites are in agreement with the expected specificity of ocriplasmin, known to cleave after positively-charged arginine or lysine residues, although P4–P3–P2 sequences here differ from the optimal substrate specificity determined for plasmin [1], with, in particular, the absence of an aromatic residue (Trp, Phe or Tyr) at position P2. X-ray structure [20] reveals that positions 166–167 and 177–178 are localized in a solvent-accessible loop, which may explain their susceptibility to autolytic cleavage. By contrast, positions 156–157 are partially buried and less accessible to solvent, which suggests that autolytic degradation requires at least partial/local unfolding, as predicted by the model proposed by Stoner et al. The validity and relevance of the latter model were further validated by looking at the effect of stabilizing agents (sucrose and mannitol) on the rate of autolysis; not only was the rate of autolysis significantly reduced in the presence of sugar, but also the ΔΔG of unfolding calculated from these data increased linearly with the concentration of stabilizing agent, as observed by others from direct measurements of protein stability [19,21,22].

Despite the existence of 3 cleavage sites, only two major autolytic species could be detected by HPLC. In addition, the HPLC profile indicates that the two species do not accumulate via parallel pathways, but instead form through a sequential process where one species appears first and is then converted into the other species. We are currently attempting to identify the exact nature of these two species in order to gain insights about the sequence of individual autolytic events.

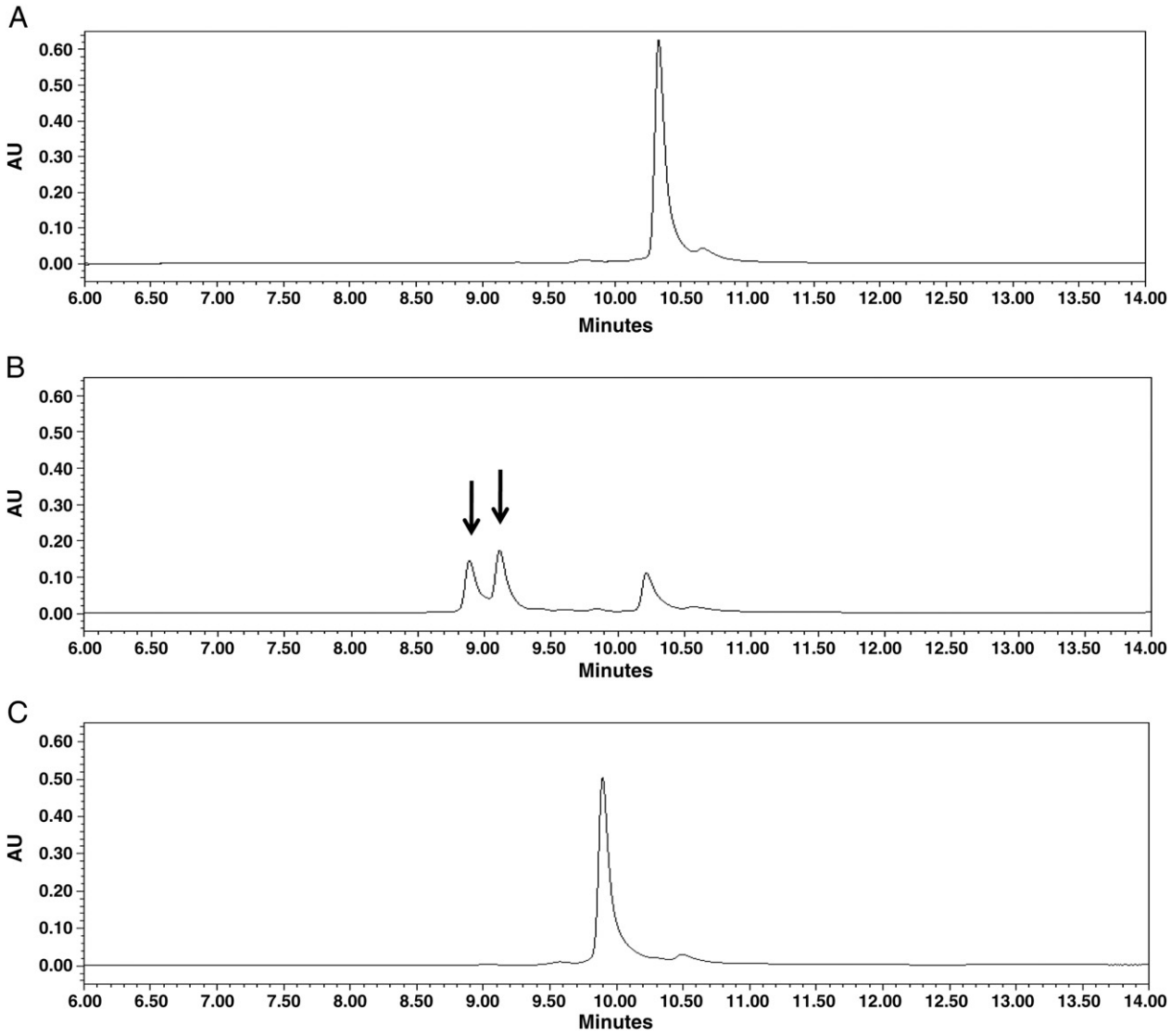

Fig. 5. Autolysis of ocriplasmin is blocked in the presence of the plasmin inhibitor D-Val-Phe-Lys chloromethyl ketone.Ocriplasmin (final concentration 18.4 μM) was incubated for 16 min at 37 °C in 25 mM sodium phosphate, pH 7.2, in the presence and absence of the plasmin inhibitor D-Val-Phe-Lys chloromethyl ketone. The samples were then analyzed by HPLC. (A) HPLC profile for a control sample kept in low-pH buffer (pH ~ 3.1). (B) HPLC profile for the sample obtained in the absence of D-Val-Phe-Lys chloromethyl ketone. The arrows indicate the autolytic species. (C) HPLC profile for the sample obtained in the presence of 1 mM D-Val-Phe-Lys chloromethyl ketone.

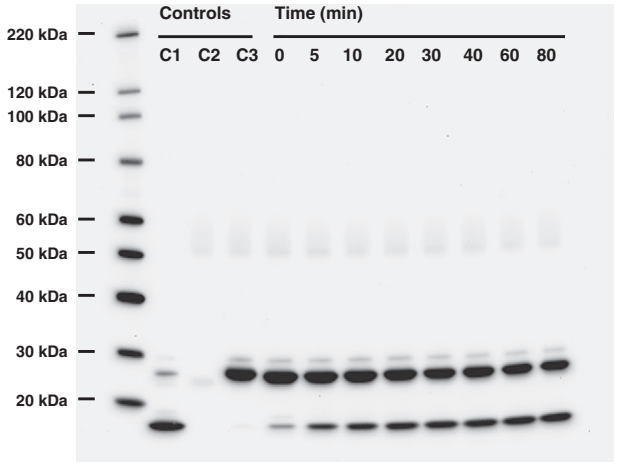

Fig. 6. Autolysis of ocriplasmin also occurs in porcine vitreous.Ocriplasmin (final concentration 18.4 μM) was added to homogenized porcine vitreous. Twenty-microliter aliquots were collected after the indicated times, and analyzed by western blot. Detection of ocriplasmin was achieved using the 7H11A11 monoclonal antibody. Lane C1 is a control where ocriplasmin was allowed to autolyze for 180 min in PBS. Lane C2 is vitreous without addition of ocriplasmin. The sample in lane C3 contained 1 mM D-Val-Phe-Lys chloromethyl ketone.

Acknowledgments

The authors wish to thank Dr Clive Long, Dr David Pearson and Dr Jean-Marie Stassen for critically reading the manuscript.

References

[1] B.J. Backes, J.L. Harris, F. Leonetti, C.S. Craik, J.A. Ellman, Synthesis of positional-scanning libraries of fluorogenic peptide substrates to define the extended substrate specificity of plasmin and thrombin, Nature Biotechnology 18 (2000) 187–193.
[2] M.S. Benz, K.H. Packo, V. Gonzalez, S. Pakola, D. Bezner, J.A. Haller, S.D. Schwartz, A placebo-controlled trial of microplasmin intravitreous injection to facilitate posterior vitreous detachment before vitrectomy, Ophthalmology 117 (2010) 791–797.
[3] O.G. Berg, P.H. von Hippel, Diffusion-controlled macromolecular interactions, Annual Review of Biophysics Chemistry 14 (1985) 131–160.
[4] R.B. Bhisitkul, Anticipation for enzymatic vitreolysis, British Journal of Ophthalmology 85 (2001) 1–3.
[5] W. Chen, W. Mo, K. Sun, X. Huang, Y.L. Zhang, H.Y. Song, Microplasmin degrades fibronectin and laminin at vitreoretinal interface and outer retina during enzymatic vitrectomy, Current Eye Research 34 (2009) 1057–1064.
[6] E.E. Clifton, The use of plasmin in humans, Annals of the New York Academy of Sciences 68 (1957) 209–229.
[7] M.D. de Smet, A. Gandorfer, P. Stalmans, M. Veckeneer, E. Feron, S. Pakola, A. Kampik, Microplasmin intravitreal administration in patients with vitreomacular traction scheduled for vitrectomy: the MIVI I trial, Ophthalmology 116 (2009) 1349–1355.
[8] C. Dommke, O. Turschner, J.-M. Stassen, F. Van de Werf, H.R. Lijnen, P. Verhamme, Thrombolytic efficacy of recombinant human microplasmin in a canine model of copper coil-induced coronary artery thrombosis, Journal of Thrombosis and Thrombolysis 30 (2010) 46–54.
[9] A. Gandorfer, E. Putz, U. Welge-Lüssen, M. Grüterich, M. Ulbig, A. Kampik, Ultrastructure of the vitreoretinal interface following plasmin assisted vitrectomy, British Journal of Ophthalmology 85 (2001) 6–10.
[10] A. Gandorfer, S. Priglinger, K. Schebitz, J. Hoops, M. Ulbig, J. Ruckhofer, G. Grabner, A. Kampik, Vitreoretinal morphology of plasmin-treated human eyes, American Journal of Ophthalmology 133 (2002) 156–159.
[11] A. Gandorfer, M. Rohleder, C. Sethi, D. Eckle, U. Welge-Lüssen, A. Kampik, P. Luthert, D. Charteris, Posterior vitreous detachment induced by microplasmin, Investigative Ophthalmology and Visual Science 45 (2004) 641–647.
[12] D.P. Han, G.W. Abrams, T.M. Aaberg, Surgical excision of the attached posterior hyaloid, Archives of Ophthalmology 106 (1998) 998–1000.
[13] M. Hermel, W. Dailey, M.K. Hartzer, Efficacy of plasmin, microplasmin, and streptokinase-plasmin complex for the in vitro degradation of fibronectin and laminin — implications for vitreoretinal surgery, Current Eye Research 35 (2010) 419–424.
[14] T. Hikichi, N. Yanagiya, M. Kado, J. Akiba, A. Yoshida, Posterior vitreous detachment induced by injection of plasmin and sulfur hexafluoride in the rabbit vitreous, Retina 19 (1999) 55–58.
[15] J. Jespersen, J. Gram, T. Astrup, The autodigestion of human plasmin follows a bimolecular mode of reaction subject to product inhibition, Thrombosis Research 41 (1986) 395–404.

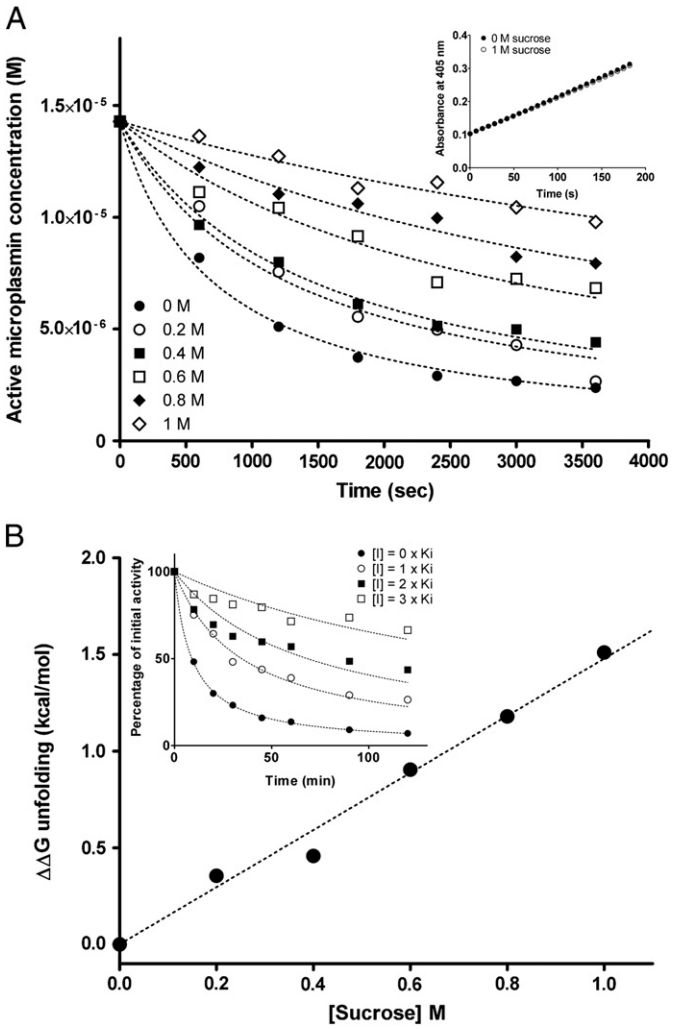

Fig. 7. The rate of ocriplasmin autolysis decreases in the presence of sucrose, supporting a model where autolysis requires unfolding.(A) Ocriplasmin (14.28 μM) was allowed to autolyze in the presence of various concentrations of sucrose. At different timepoints, aliquots were collected and the concentration of active enzyme was calculated from the measure of residual hydrolytic activity. Second order rate constants for autolysis were obtained by fitting the data with Eq. (2) (dotted lines). The inset shows initial rates of S-2403 (0.3 mM) hydrolysis recorded in the absence and presence of 1 M sucrose. (B) $\Delta\Delta G_{unfolding}$ for individual sucrose concentrations were calculated from (A) with the help of Eq. (3) and plotted as a function of sucrose concentration. The inset shows the effect of benzamidin on ocriplasmin autolysis. Ocriplasmin concentration was 14.7 μM. The dotted lines were drawn to aid visualization. All experiments were conducted at 37 °C in 25 mM sodium phosphate pH 7.2.

[16] X. Li, X. Shi, J. Fan, Posterior vitreous detachment with plasmin in the isolated human eye, Graefe's Archive for Clinical and Experimental Ophthalmology 240 (2002) 56–62.
[17] F. Markwardt, H. Landmann, P. Walsmann, Comparative studies on the inhibition of trypsin, plasmin, and thrombin by derivatives of benzylamine and benzamidine, European Journal of Biochemistry 6 (1968) 502–506.
[18] N. Nagai, E. Demarsin, B. Van Hoef, S. Wouters, D. Cingolani, Y. Laroche, D. Collen, Recombinant human microplasmin: production and potential therapeutic properties, Journal of Thrombosis and Haemostasis 1 (2003) 307–313.
[19] T.F. O'Connor, P.G. Debenedetti, J.D. Carbeck, Stability of proteins in the presence of carbohydrates; experiments and modeling using scaled particle theory, Biophysical Chemistry 127 (2007) 51–63.
[20] M.A. Parry, C. Fernandez-Catalan, A. Bergner, R. Huber, K.P. Hopfner, B. Schlott, K.H. Gührs, W. Bode, The ternary microplasmin–staphylokinase–microplasmin complex is a proteinase–cofactor–substrate complex in action, Nature Structural Biology 5 (1998) 917–923.
[21] N.K. Poddar, Z.A. Ansari, R.K. Brojen Singh, A.A. Moosavi-Movahedi, F. Ahmad, Effect of monomeric and oligomeric sugar osmolytes on DeltaGD, the Gibbs energy of stabilization of the protein at different pH values: is the sum effect of monosaccharide individually additive in a mixture? Biophysical Chemistry 138 (2008) 120–129.

[22] Z. Saadati, L. Asadi, S. Larki, Thermal stability of α-Lactalbumin in the presence of various sugars as osmolytes, Journal of Physical and Theoretical Chemistry of Islamic Azad University of Iran 7 (2010) 165–172.
[23] J. Sebag, Pharmacologic vitreolysis, Retina 18 (1998) 1–3.
[24] G.-Y. Shi, H.-L. Wu, Differential autolysis of human plasmin at various pH levels, Thrombosis Research 51 (1988) 355–364.
[25] P. Sriram, N. Kalogerakis, L.A. Behie, Experimental determination of the rate of autolysis of trypsin at 37 °C, Biotechnology Techniques 10 (1996) 601–606.
[26] M.R. Stoner, D.A. Dale, P.J. Gualfetti, T. Becker, M.C. Manning, J.F. Carpenter, T.W. Randolph, Protease autolysis in heavy-duty liquid detergent formulations: effects of thermodynamic stabilizers and protease inhibitors, Enzyme and Microbial Technology 34 (2004) 114–125.
[27] M.T. Trese, Enzymatic vitreous surgery, Seminars in Ophthalmology 15 (2000) 116–121.
[28] M.T. Trese, Enzymatic-assisted vitrectomy, Eye 16 (2002) 365–368.
[29] J.F. Vander, R. Kleiner, A method for induction of posterior vitreous detachment during vitrectomy, Retina 12 (1992) 172–173.
[30] T.C. Verstraeten, C. Chapman, M. Hartzer, B.S. Winkler, M.T. Trese, G.A. Williams, Pharmacologic induction of posterior vitreous detachment in the rabbit, Archives d'Ophtalmologie 111 (1993) 849–854.
[31] J. Whitefleet-Smith, E. Rosen, J. McLinden, V.A. Ploplis, M.J. Fraser, J.E. Tomlinson, J.W. McLean, F.J. Castellino, Expression of human plasminogen cDNA in a baculovirus vector-infected insect cell system, Archives of Biochemistry and Biophysics 271 (1989) 390–399.
[32] H.-L. Wu, G.-Y. Shi, M.L. Bender, Preparation and purification of microplasmin, Proceedings of the National Academy of Sciences of the United States of America 84 (1987) 8292–8295.